American Mineralogist, Volume 89, pages 1192–1201, 2004

The effect of elevated methane pressure on methane hydrate dissociation

SUSAN CIRCONE,* LAURA A. STERN, AND STEPHEN H. KIRBY

U.S. Geological Survey, 345 Middlefield Road MS 977, Menlo Park, California 94025, U.S.A.

ABSTRACT

Methane hydrate, equilibrated at *P*, *T* conditions within the hydrate stability field, was rapidly depressurized to 1.0 or 2.0 MPa and maintained at isobaric conditions outside its stability field, while the extent and rate of hydrate dissociation was measured at fixed, externally maintained temperatures between 250 and 288 K. The dissociation rate decreases with increasing pressure at a given temperature. Dissociation rates at 1.0 MPa parallel the complex, reproducible *T*-dependence previously observed between 250 and 272 K at 0.1 MPa. The lowest rates were observed near 268 K, such that >50% of the sample can persist for more than two weeks at 0.1 MPa to more than a month at 1 and 2 MPa. Varying the pressure stepwise in a single experiment increased or decreased the dissociation rate in proportion to the rates observed in the isobaric experiments, similar to the rate reversibility previously observed with stepwise changes in temperature at 0.1 MPa.

At fixed *P*, *T* conditions, the rate of methane hydrate dissociation decreases monotonically with time, never achieving a steady rate. The relationship between time (*t*) and the extent of hydrate dissociation is empirically described by:

$$\text{Evolved gas (\%)} = A \cdot t^{B} \quad (1)$$

where the pre-exponential term *A* ranges from 0 to 16% s^{-B} and the exponent *B* is generally <1. Based on fits of the dissociation results to Equation 1 for the full range of temperatures (204 to 289 K) and pressures (0.1 to 2.0 MPa) investigated, the derived parameters can be used to predict the methane evolution curves for pure, porous methane hydrate to within ±5%. The effects of sample porosity and the presence of quartz sand and seawater on methane hydrate dissociation are also described using Equation 1.

INTRODUCTION

Methane hydrate, $CH_4 \cdot nH_2O$ with $n \geq 5.75$, belongs to a family of nonstoichiometric, crystalline compounds in which hydrogen-bonded water molecules form a framework of polyhedral cavities occupied by "guest" molecules such as methane. Methane gas forms a structure I (sI) hydrate in which the unit cell consists of 46 H_2O and up to 8 CH_4 molecules occupying both small (pentagonal dodecahedral) and large (tetrakaidecahedral) cavities in a ratio of 1:3. In naturally occurring sI gas hydrates, CH_4 is typically the principal "guest" molecule, with various other alkanes and inorganic gases such as N_2, H_2S, and CO_2 present in minor amounts. All natural samples recovered by drill core from both marine continental margin sediments and permafrost environments undergo some degree of dissociation, making the determination of the original hydrate composition impossible without independent knowledge of the in situ phase assemblage. While the phase equilibria of CH_4 hydrate, which is stable over a range of elevated pressure and low temperature conditions, has been investigated in detail (see Sloan 1998, for a summary of the published phase equilibria data), studies of CH_4 hydrate dissociation rates, and for that matter any hydrate, are few.

Previous studies reported incomplete dissociation of sI CH_4 hydrate at 0.1 MPa and temperatures below 273 K. In experiments where synthetic CH_4 hydrate was heated from below 193 K (the hydrate equilibrium boundary at 0.1 MPa), partial dissociation occurred below 250 K (Davidson et al. 1986; Handa and Stupin 1992). The remaining gas was released at the H_2O melting point (for ice Ih, 273 K, henceforth "ice melting point"). Visual observation of CH_4-rich hydrates recovered from drill core indicated that dissociation can stall at *P*, *T* conditions well outside the hydrate stability field (e.g., Dallimore and Collett 1995). However, a CH_4-rich sI marine hydrate sample, finely ground after recovery and stored in liquid nitrogen, dissociated completely by 220 K (Handa 1988). Ershov and Yakushev (1992) and Yakushev and Istomin (1992) reported that synthetic CH_4 hydrate could persist in varying states of partial preservation following depressurization at temperatures below the ice point. The extent of preservation ranged from >90% after depressurization to a few percent after several days to more than a year. They, along with others (e.g., Davidson et al. 1986; Handa 1986), suggested that the ice produced by dissociation forms a film on the hydrate particle, presenting an impermeable boundary to gas diffusion that results in "self preservation" of the hydrate.

We previously reported on a series of experiments involving CH_4 hydrate ($CH_4 \cdot 5.89\ H_2O$), in which samples were equilibrated at specific *P* and *T* conditions in the hydrate stability field, then were rapidly depressurized to 0.1 MPa and monitored continu-

* E-mail: scircone@usgs.gov

ously for gas release. We identified three distinct regimes of dissociation behavior over discrete temperature intervals above the equilibrium boundary. Dissociation rates were similar and increased monotonically with increasing T at 204–240 K and above 272 K, although hydrate dissociated to gas + ice at low T and gas + water at temperatures above the ice melting point. However, in the intermediate T interval of 242–272 K, dissociation rates were depressed up to several orders of magnitude and varied complexly but reproducibly with temperature (Stern et al. 2001, 2003). Thus, while 90–100% of a ~30 g sample dissociated in a few minutes to a few hours at both low and high T, in the intermediate T range at least half of the sample persisted for a few hours to several tens of hours. At the optimum preservation temperature of 268 K, which is 75 K above the CH_4 hydrate stability boundary, more than half of the sample persisted for two weeks at 0.1 MPa. While Ershov and Yakushev (1992) have termed any persistence of hydrate as "self preservation," regardless of the amount, we use "anomalous preservation" to describe the depressed dissociation rates and persistence of >10% of the sample for hours to weeks in samples subjected to rapid depressurization at isothermal conditions between 242 and 272 K (Stern et al. 2001). This terminology was chosen to distinguish such preservation from the persistence of <10% of the hydrate following other P, T pathways, such as rapid depressurization at T < 240 K or warming of the sample from 188 to 272 K at 0.1 MPa. This final fraction of hydrate can persist for more than a year (Ershov and Yakushev 1992), but dissociates rapidly as T approaches the ice melting point.

In this study we report on the effect of pressure on CH_4 hydrate dissociation rates, specifically the effect of 1.0 and 2.0 MPa CH_4 pressure on the dissociation rate at various temperatures and the effect of stepwise changes in pressure on a dissociating sample. We also apply an empirical equation to describe the extent and rate of dissociation with time for CH_4 hydrate under a wide range of P, T conditions. The principal effects of temperature, pressure, sample composition (the addition of quartz sand and seawater), and porosity are summarized. Lastly, the phenomena of anomalous preservation of CH_4 hydrate and experimental constraints on its possible causes are revisited.

Experimental method

Methane hydrate samples were synthesized, using the method and apparatus described by Stern et al. (1996, 2001), in a pressure vessel from nominally 26 g of granulated H_2O ice (180 to 250 μm grain size) and pressurized CH_4 gas (see Fig. 1). Hydrate synthesis occurred as the reactants were heated from 250 to 290 K while CH_4 pressure increased from 25 to 31 MPa due to heating under approximately constant volume conditions. The reaction reached completion at 290 K, where isothermal conditions were maintained for 30 to 48 h while pressure slowly decreased as synthesis proceeded. Complete reaction of all H_2O to hydrate was confirmed by the absence of abrupt increases in pressure or temperature as samples were cooled through the H_2O solid-liquid boundary. Occasionally, when a freezing signal was detected, the heating cycle was repeated until no P, T discontinuity was observed. The measured composition of CH_4 hydrate synthesized at these conditions is $CH_4 \cdot 5.89\ H_2O$, with a precision of ±0.01 (5 samples) and an accuracy of ±0.06 (±1 mol% of CH_4 gas; Circone et al. 2001).

After synthesis, samples were equilibrated at a constant temperature (T_{ext}) maintained by an external fluid bath surrounding the pressure vessel. Pressure was then decreased from post-synthesis conditions to a pressure at least 2 MPa above the equilibrium boundary. Hydrate dissociation was initiated by rapidly decreasing the CH_4 pressure to conditions outside the hydrate stability field (Fig. 2). The depressurization was performed in ~15 s to 0.1 MPa, or in 10–35 s to 1.0 or 2.0 MPa pressure, by venting CH_4 gas from the system (at time = 0 h in Figs. 3 and 4). The sample was then opened to a flow meter, which collected the released gas from the dissociating hydrate sample. Internal sample temperatures were monitored during dissociation by one or four thermocouples (positions shown in Fig. 1, results in Figs. 3a and 4a).

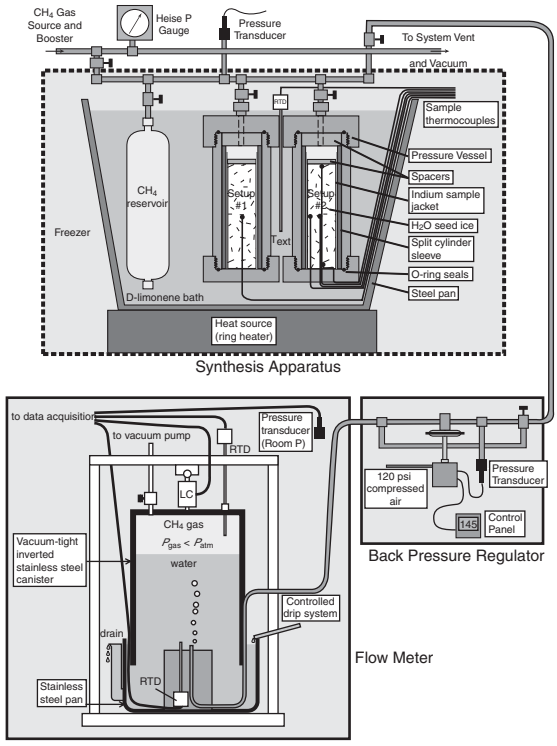

Figure 1. Schematic diagram (not to scale) of synthesis apparatus, back pressure regulator, and flow meter apparatus. Two hydrate samples were synthesized simultaneously in stainless steel pressure vessels. One sample has an axially and radially centered internal thermocouple, and the second has four internal thermocouples, three centered along the sample axis and one axially centered at the sample side. The flow meter determined the amount of gas released through dissociation by monitoring the change in weight of an inverted, water-filled, close-ended cylinder as the released gas displaced the water. The cylinder was partially immersed in a pan of water that was open to the atmosphere, and a constant water level was maintained by a continuous drip system, such that the effect of cylinder buoyancy on the measured weight was constant. The flow meter had a gas capacity of 7 L at ambient conditions and can measure gas release rates ranging over more than four orders of magnitude (3000 mL/min to less than 0.1 mL/min). Details of flow meter operation have been reported previously (Circone et al. 2001). The back pressure regulator maintained a constant, elevated pressure on the sample, while the flow meter operated at 0.1 MPa (see text).

The amounts and rates of dissociation were measured using our custom flow meter (Fig. 1; Circone et al. 2001). Gas yields were typically within ±5 mol% of that expected, with somewhat larger deviations observed at the highest measured dissociation rates, either from incomplete venting of the pore gas before the valve was closed (producing high yields) or from the onset of dissociation during depressurization (producing low yields). In short-duration experiments of up to 30 h the loss of CH_4 from solution in water in the flow meter was negligible. However, CH_4 solution does decrease the measured gas yields when the drip system is operated continuously for longer time intervals (Circone et al. 2001). This problem was circumvented by collecting data with the flow meter only while operating the drip system for short intervals (typically ≤1 h) periodically every one or more days (Fig. 3b).

For dissociation experiments performed at elevated pressures, a back pressure regulator (Tescom Model ER 3000), located between the sample and the flow meter

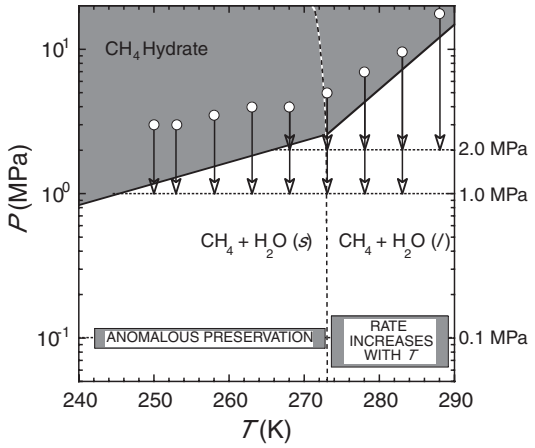

FIGURE 2. Starting *P*, *T* conditions for dissociation of CH_4 hydrate following rapid depressurization to 1.0 or 2.0 MPa. The gray-shaded region defines the CH_4 hydrate stability field. The vertical dashed curve shows the H_2O ice-liquid boundary. The dissociation behavior for CH_4 hydrate depressurized to 0.1 MPa has been described previously (e.g., Stern et al. 2001, 2003). All experiments started at a pressure ~2.0 MPa above the equilibrium boundary, except one at 288 K and 2.0 MPa, which was depressurized from ~6 MPa above the boundary.

(Fig. 1), maintained the pressure in the sample vessel to within ±0.03 MPa of the set point by releasing gas to the flow meter as the hydrate dissociated. Constant pressure was maintained continuously in long-duration experiments, although gas-flow measurements with the flow meter were intermittent. The back pressure regulator exhibited some hysteresis at the slowest dissociation rates (Fig. 3a), producing some variation in the pressure that does not occur at higher rates (Fig. 4a).

Experiments were performed at 5 K intervals from 253 to 283 K at 1.0 MPa and 268 to 288 K at 2.0 MPa, as well as one at 250 K, 1.0 MPa (Fig. 2). The low temperature limit of these experiments was fixed by the CH_4 hydrate equilibrium boundary. Additional experiments were also performed at 0.1 MPa and select temperatures to permit direct comparison with the dissociation rates measured at elevated pressures (see below).

RESULTS

The effect of temperature on hydrate dissociation behavior at elevated CH_4 pressure was similar to that observed at 0.1 MPa (Stern et al. 2001, 2003). At 1.0 or 2.0 MPa and isothermal conditions between 253 and 268 K, the rate of gas evolution changed over time (Fig. 3b). In the first hour after rapid depressurization, the initial dissociation rate was high, then decreased to progressively slower rates. At least half of the sample persisted for two weeks or more in this temperature range. The remaining hydrate was dissociated by heating the sample to 282 K; the gas was released in a single, well-defined event near 273 K (Fig. 3c). At 2.0 MPa, experiments were performed only at 268 K. The dissociation rates were depressed below those at 1.0 MPa, although the initial gas release in the first hour was greater (see below). At 250 K and 1.0 MPa (not shown), the experimental conditions were near the transition in behavior that defines the anomalous preservation regime (Stern et al. 2001, 2003). Thus, the initial dissociation rate was sufficiently high to release half of the gas content in 1.3 h before the sharp decrease in dissociation rate was observed.

At bath temperatures above the ice melting point, hydrate dissociation occurred rapidly (Fig. 4), such that samples dissociated completely in a matter of hours (1 hour at 283 K and 1.0 MPa to ~20 h at 273 K and 2.0 MPa), and again the dissociation

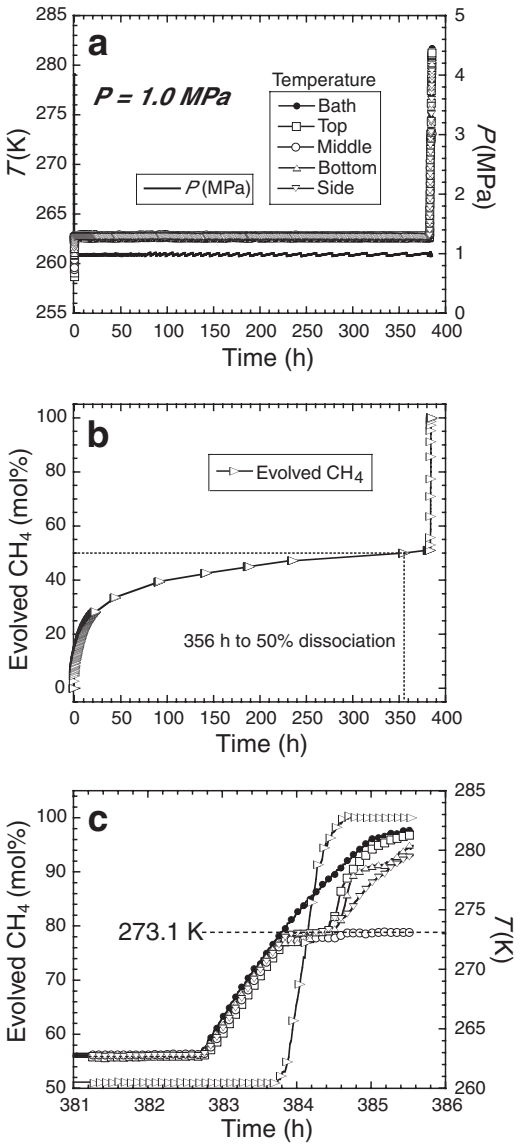

FIGURE 3. Dissociation behavior of CH_4 hydrate at elevated pressure and at temperatures in the anomalous preservation regime ($T < 273$ K). (**a**) *P*, *T* conditions for an experiment performed at 263 K, 1.0 MPa. Depressurization of the sample from 4 to 1 MPa resulted in adiabatic cooling and produced the temperature decrease at time = 0 h; the sample equilibrated with the external bath *T* within minutes. After 383 h at 263 K, the sample was warmed to 282 K to release the remaining gas from the sample. The pressure record, essentially isobaric for the first 75 h, shows small fluctuations (±0.03 MPa, the precision of the back pressure regulator) with increasing period as the dissociation rate decreases over time. (**b**) Evolution of CH_4 gas from the sample over time. Data were collected periodically every 1 to 5 days after an initial 23 h of continuous data collection (see text). Half of the gas content of the hydrate sample was released after 356 h. (**c**) The release of the remaining gas after heating the sample through 273 K, and the internal sample temperature history. Sample temperatures remain buffered just below 273 K as dissociation proceeds, rising to the ice melting point (273.08 K at 1.0 MPa) as gas evolution ceases (see Circone et al. 2004 for further details). In all panels, every 5th data point is plotted, except no symbols are plotted for *P* in **a**. Uncertainty in evolved gas is ±1%.

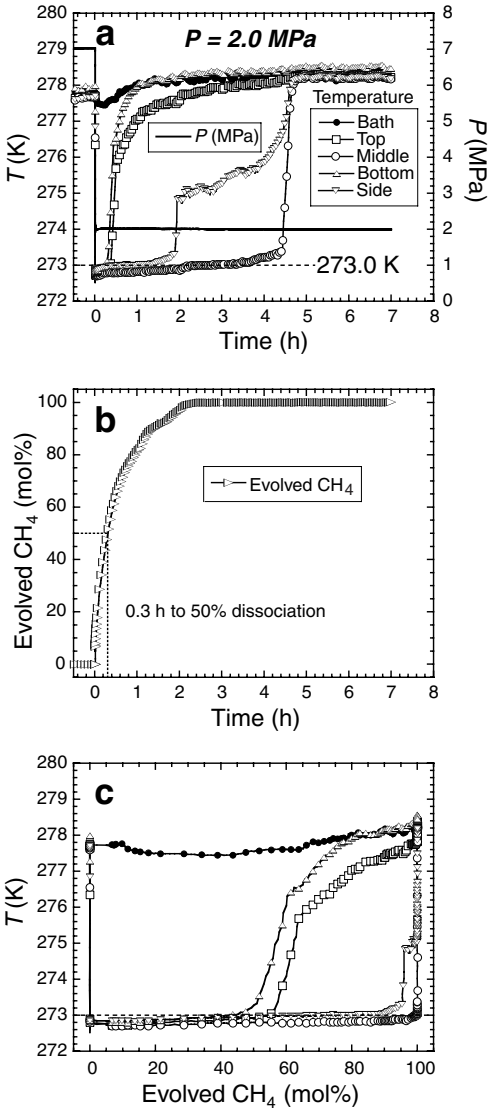

FIGURE 4. Dissociation behavior of CH_4 hydrate at elevated pressure and at temperatures above the ice melting point. (**a**) *P*, *T* conditions for an experiment performed at 278 K, 2.0 MPa. The temperature decrease at time = 0 h is due to adiabatic cooling of the sample from depressurization and endothermic hydrate dissociation. Internal sample temperatures were depressed more than 4 K for up to 4.4 h, while the external bath *T* remained approximately isothermal near 278 K. (**b**) The evolution of CH_4 gas from the sample over time. Half of the gas content of the hydrate sample was released in 19 minutes, and gas evolution ceased after 2.6 h. (**c**) The relationship between gas release and internal sample temperature. All sample temperatures were buffered below 273 K until half of the gas was released, then the temperature at the sample top and bottom rebounded toward T_{ext}. The sample side and middle remained buffered below 273 K until the reaction neared completion, at which point temperatures rose to 273.0 K (the ice melting point at 2.0 MPa), before finally rebounding to T_{ext}. In all panels, every 5th data point is plotted, except no symbols are plotted for *P* in **a**. Uncertainty in evolved gas is ±2%.

rate decreased continuously over time (Fig. 4b). Furthermore, although the external bath temperature remained approximately isothermal, the internal sample temperatures were consistently buffered just below 273 K as dissociation proceeded (Figs. 4a and 4c). This phenomenon, discussed in detail in Circone et al. (2004), was observed at both 0.1 MPa and elevated pressures. It is thought to arise from the freezing of the water produced by the strongly endothermic hydrate dissociation reaction (hydrate to gas + water). The temperature offset from the pure melting point of H_2O arises from solution of the released hydrate-forming gas in the water, producing a depression of the freezing point. This thermal buffering behavior was also observed when samples are heated through 273 K (Fig. 3c).

The effect of pressure on dissociation rate is evident when gas evolution curves are compared for experiments conducted at 268 K (Fig. 5). Curves 1 and 2 show the dissociation behavior at a constant pressure of 0.1 MPa and indicate that depressurization rate is not a strong factor affecting the dissociation rates (see caption). Curves 3 and 4 show the effect of elevated pressure on dissociation for experiments at 1.0 and 2.0 MPa, respectively. At 1.0 MPa, the initial amount of gas released is smaller and the slope of the gas release curve is shallower. At 2.0 MPa, the slope is even shallower, although the initial gas release event in the first hour following depressurization may be larger (Fig. 5a), based on two experiments at 2.0 MPa that showed this large, initial gas release. One sample was initially depressurized to 0.1 MPa, allowed to partially dissociate for 0.2 h, and then repressurized to 2.0 MPa (curve 5). This experiment showed that dissociation rates are high in the first hour, remain high compared to those of a sample directly depressurized to 2.0 MPa, but eventually converge after the first 100 h. Lastly, after dissociating for >200 h at 2.0 MPa, decreasing pressure to 0.1 MPa resulted in an increase in dissociation rate by more than a factor of 10 (curves 4 and 5). When repressurized to 2.0 MPa (curve 4), the rate again slows, approaching the previous 2.0 MPa rate. Similar changes in dissociation rate were observed in another experiment in which *P* was varied from 2.0 to 1.0 to 2.0 MPa (not shown). This ability to increase and decrease the dissociation rate by changing the pressure is comparable to the rate reversibility with changing temperature in the anomalous preservation regime at 0.1 MPa (Stern et al. 2003, Fig. 2).

DISCUSSION

Summary of dissociation behavior

In our previous work we compared dissociation rates of CH_4 hydrate at different temperatures and 0.1 MPa CH_4 pressure. Because dissociation rates vary with time and extent of dissociation, we compared the average dissociation rate calculated from the time needed to release 50% of the gas content of the sample (Fig. 6; see Stern et al. 2001, 2003). The anomalous preservation regime is defined by average dissociation rates that are depressed up to four orders of magnitude below those that occur at lower and higher temperatures. At 0.1 MPa, this anomalous dissociation behavior occurs between 240 and 273 K, with the slowest rates observed at 268 ± 0.5 K. At elevated pressures, dissociation rates are depressed further and the complex temperature-dependency parallels that observed at 0.1 MPa. In fact, experiments at 253 and 268 K exhibited such slow dissociation rates that samples had not released 50% of their gas content after more than 36 days at isothermal conditions. At temperatures above the ice melting

point, average dissociation rates are also depressed at elevated pressures relative to those at 0.1 MPa.

The dissociation rate of CH_4 hydrate is more completely described by determining the rate as it evolves over time. As shown in Figures 3b and 4b, porous CH_4 hydrate does not dissociate at a constant rate, as evidenced by the continually changing slope of the curves. Instead, the rate decreases continuously and exponentially. At 0.1 MPa (Fig. 7), the time scales of the experiments and the observed dissociation rates are comparable both below 240 K (Fig. 7a) and above 273 K (Fig. 7b). Increasing T_{ext} shifted dissociation to higher rates and shorter time scales. However, there are important differences. At the lower

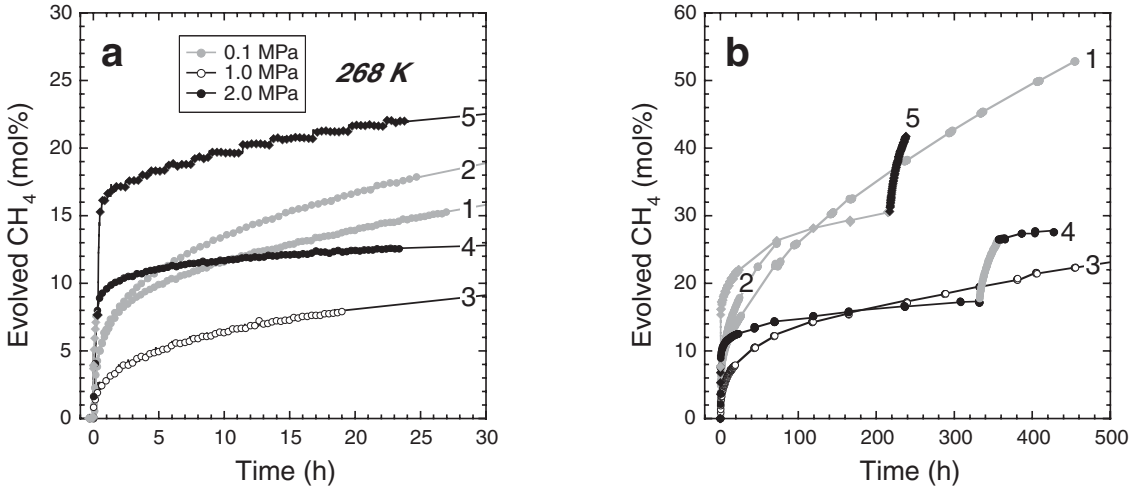

FIGURE 5. Dissociation of CH_4 hydrate samples depressurized to, and held at, various pressures between 0.1 and 2.0 MPa while maintained isothermally within 0.5 K of 268.0 K. Slopes of curves reflect the rate of dissociation (in mol%/h), symbol shading indicates pressure during dissociation (see legend), and every tenth data point has been plotted. (**a**) The first 30 h of dissociation. (**b**) The complete, isothermal portions of the experiments, with the exception of curve 3, which was maintained for 862 h at isothermal, isobaric conditions. Curves 1 and 2 show the results of two experiments at 0.1 MPa, in which the sample was depressurized quickly (3.1 to 0.1 MPa in 21 s, curve 1) or slowly (2.3 to 0.1 MPa in 12.6 min, curve 2). Sample-to-sample differences in dissociation rates at the same *P*, *T* conditions, especially after the first 24 h of dissociation, are small compared to the effects of changing temperature and pressure (see text). Curve 3 shows the results at 1.0 MPa, in which the sample released just 28% of its gas content after 862 h. Curve 4 shows the results of an experiment initially held at 2.0 MPa for 332 h, then depressurized to 0.1 MPa and held for 25 h before pressurizing to 2.0 MPa again. By the end of the isothermal hold at 428 h, the dissociation rate approached that observed before the decrease to 0.1 MPa. Curve 5 (diamond symbol) shows an experiment initially depressurized to 0.1 MPa and held for 0.26 h, before pressurizing to 2.0 MPa. After 217 h, the pressure was again decreased to 0.1 MPa. Uncertainties in gas yields range from ±1 (curves 2, 4, 5) to ±3% (curves 1, 3).

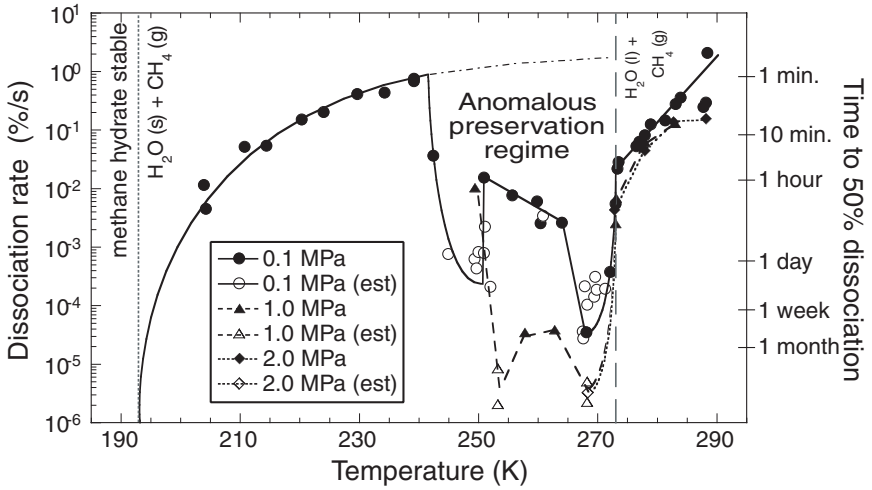

FIGURE 6. Average rate of dissociation of CH_4 hydrate at various temperatures, based on the time required to dissociate 50% of the sample following rapid depressurization to 0.1, 1.0, or 2.0 MPa (modified from Stern et al. 2001, 2003). Each data point represents an experiment performed at a single temperature and pressure; all experiments were equilibrated at conditions within the hydrate stability field prior to depressurization. Solid symbols indicate that the sample reached at least 50% dissociation while isothermal conditions were maintained, and open symbols indicate that the time to 50% dissociation was estimated from a linear extrapolation of the last few hours of isothermal data. At 1.0 MPa and 253 or 268 K, two estimated average rates are shown for a linear extrapolation to 50% dissociation (faster rates) and for a power law extrapolation of the entire data set (slower rates, see text). Uncertainties in rate are within ±7%, with plotted symbol height corresponding to ±20%.

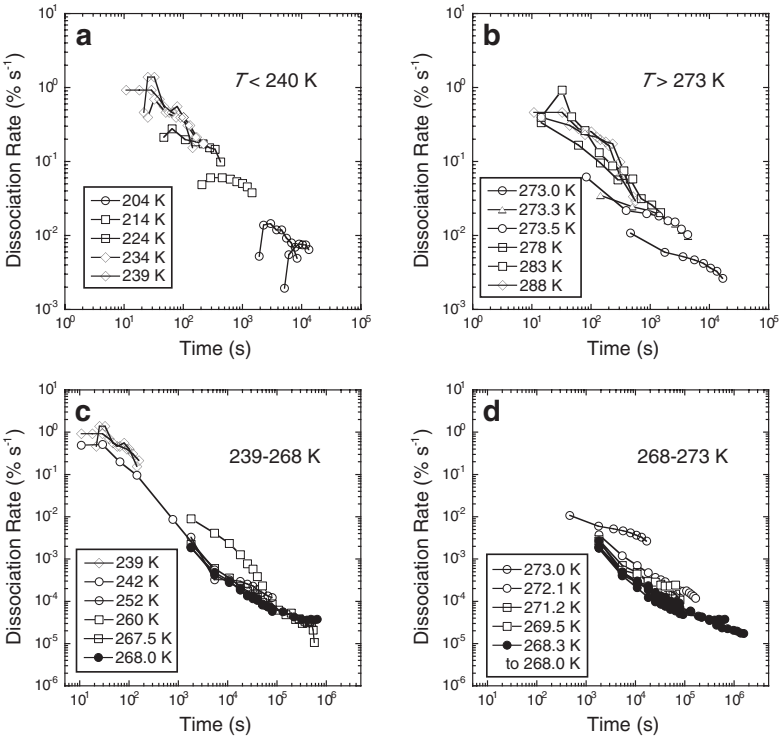

FIGURE 7. A sampling of CH_4 hydrate dissociation rates at 0.1 MPa and various temperatures. Rates have been calculated for several intervals in a given experiment to illustrate the evolution of the dissociation rate over time. Because of the difference in time scale for the various experiments, dissociation rates were calculated in one of two ways; in both cases the *x*-axis is plotted at the midpoint in time for the dissociation interval of interest. In experiments performed below 240 K (**a**) and at or above 273 K (**b**), dissociation rates were calculated for 10% increments up to 80% dissociation. The curves are shifted to shorter times as temperature increases because the time to reach 10, 20, 30% dissociation and so on is decreasing as the rate increases. Note that, as the extent of dissociation exceeds 80%, the rates drop off significantly as the last remaining gas is released from the sample (not shown). In experiments within the anomalous preservation regime (**c** and **d**), dissociation rates were calculated for set time intervals because dissociation rates are orders of magnitude slower (0–2 h in 1 hour steps, 2–12 h in 2 hour steps, 12–24 h in 4 hour steps, then periodically as data collected. See Fig. 3b). Uncertainties in rate are within ±7%, with plotted symbol height corresponding to ±10%.

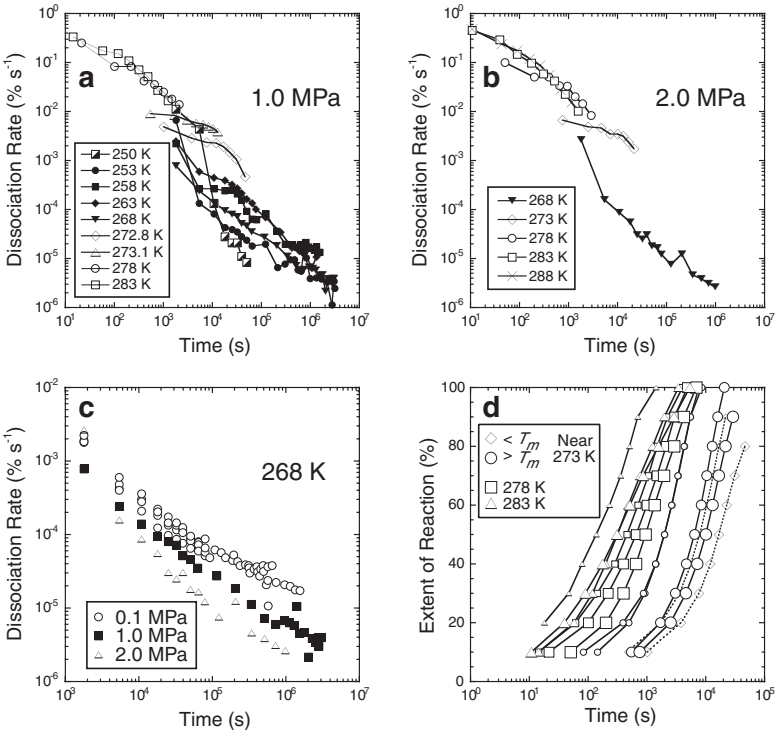

FIGURE 8. The evolution of CH_4 hydrate dissociation rates at various temperatures and 1.0 or 2.0 MPa (**a** and **b**), comparison of the rates at 268 K and various pressures (**c**), and comparison of the extents of reaction with time at temperatures near or above the ice melting point (T_m) (**d**). As in Figure 7, rates in (**a**–**c**) have been calculated in two ways depending on the time scale of the experiment. (**a**) shows that the dissociation rates at 1.0 MPa followed a similar distribution depending on whether conditions are in the anomalous preservation regime or above 273 K. The onset *T* of the anomalous preservation regime at 1.0 MPa is shifted to 250 K. While more than half of the sample (56%) dissociated in 2.0 h, only 2% more of the gas content was released after an additional 17 h. At 253 K, similar behavior was observed, but the initial gas release was much less (24% in 2 h) and the rate quickly decreased by two orders of magnitude. The rates increased with increasing temperature, except for the decrease at 268 K. **b** shows that at 2.0 MPa, rates at 268 K are again several orders of magnitude below those at warmer temperatures. **c** shows that the dissociation rates at 268 K decrease with increasing pressure in a predictable and systematic manner. **d** compares the time intervals required to release CH_4 gas from the samples in 10% increments, showing the effect of temperature (in 5 K increments at 273, 278, and 283 K) and pressure on the inferred dissociation rates (dissociation rates at higher temperatures are difficult to differentiate in panels **a** and **b**). Symbol size increases with increasing pressures of 0.1, 1.0, and 2.0 MPa. Uncertainties in rate are within ± 7%, with plotted symbol height corresponding to ±10%.

temperatures, hydrate dissociated to ice + gas in hours to minutes as T_{ext} increased. Sample temperatures became depressed below T_{ext} in proportion to the rate of the endothermic reaction. Dissociation was incomplete, and the remaining 5–10% of the gas was released as the samples were warmed, culminating in a final pulse of gas as temperatures reached the ice melting point. Above the ice melting point (Fig. 7b), the *T* effect was greater and the dissociation rates climbed quickly with increasing T_{ext}. In this regime hydrate dissociated to gas + water (Circone et al. 2004), and dissociation proceeded to completion.

In the anomalous preservation regime, in which hydrate dissociated to ice + gas, dissociation occurred at slower rates and over longer time scales (Figs. 7c,d) while in thermal equilibrium with the external bath. The transition in dissociation behavior at lower *T* is apparent in the 242 K experiment, where the initial gas release was rapid and exceeded 50% in 0.38 h, but then the rate dropped significantly (Fig. 7c). The effect of temperature on dissociation rates is complex, as the rates are comparable near 250 and 268 K but higher between 256 and 264 K (Fig. 6, 260 K experiment in Fig. 7c). While the extent of dissociation was greater at these intermediate temperatures (>50% in 5 h), rates were still suppressed relative to those outside the anomalous preservation regime. At 268.0 ± 5 K, the observed rates reached a minimum, then increased with increasing T_{ext} up to the ice melting point (Fig. 7d).

At elevated pressures, the temperature dependency of dissociation rates was much the same as that at 0.1 MPa. The onset temperature for the anomalous preservation regime at 1.0 MPa occurred at higher temperature than at 0.1 MPa (Fig. 6), near 250 K (Fig. 8a). As T_{ext} increased in approximately 5 K increments, the dissociation rates increased between 250 and 273 K, except for the abrupt decrease at 268 K. At 1.0 MPa (Fig. 8a) and 2.0 MPa (Fig. 8b), the rates increased and the time scales of the experiments decreased exponentially at *T* above 268 K.

The effect of pressure on the dissociation rate is straightforward at 268 K (Fig. 8c) and higher temperatures (Fig. 8d). Dissociation rates decreased systematically with increasing pressure, although at 268 K, some variability was observed in the initial dissociation rate. This effect of pressure on dissociation rate was expected, since the volume change upon dissociation was large and positive due to the formation of the CH_4 gas phase, and thus increasing pressure decreases the driving force for dissociation (Le Châtelier's Principle). Of great interest is the fact that the anomalous dissociation behavior persisted at elevated pressure and is not an artifact of rapid depressurization to 0.1 MPa. Two experiments performed just below the ice melting point at 0.1 and 1.0 MPa (diamonds, Fig. 8d) illustrate the large effect that small changes in temperature have on the dissociation rates within 0.5 K of the ice melting point. The dissociation rate is highly sensitive to temperature, depending on whether hydrate is dissociating to gas + ice ($T < T_m$) or gas + water ($T > T_m$).

Lastly, increasing intergranular porosity in the hydrate, adding quartz sand, and partially saturating the hydrate with seawater in dissociation experiments performed at 0.1 MPa affected the dissociation curves and rates in a predictable manner (Fig. 9). Near 268 K, the dissociation rate of CH_4 hydrate increased with increasing intergranular porosity (from ~30 to ~50%). The dissociation rate also increased as hydrate-hydrate grain contacts

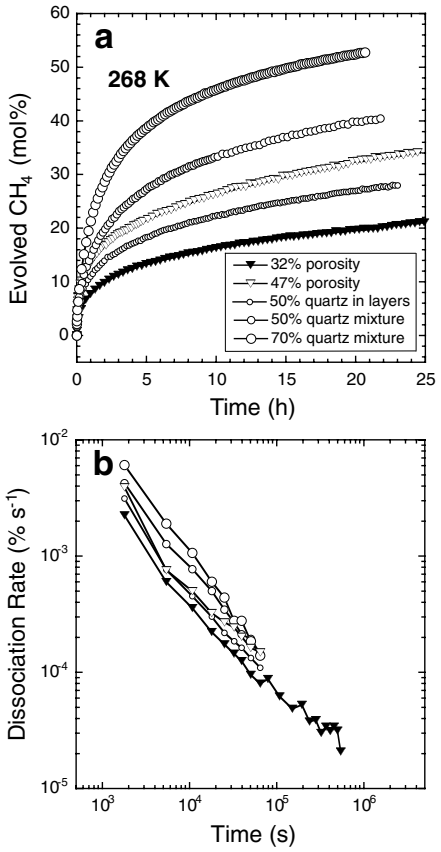

FIGURE 9. The effect of hydrate porosity and quartz sand on the dissociation of porous methane hydrate at 268 K and 0.1 MPa. Panel **a** shows the methane evolution curves over time, with every 10th data point plotted. Only one low-porosity sample was plotted for comparison. (**b**) Calculated rates for these experiments. Dissociation rates have converged after 24 h, as indicated by the near parallel curves by this time in **a**.

were disrupted by the addition of quartz, first as discrete layers (50% by volume, 4 layers hydrate:3 layers quartz), and then as homogeneous mixtures with increasing quartz content (details on sample synthesis in Stern et al. 2000). The partial saturation of pores with seawater increased the dissociation rate at warm *T* (see Circone et al. 2004 for details).

Modeling CH_4 hydrate dissociation behavior

When CH_4 hydrate is placed in *P*, *T* conditions outside its stability field, dissociation generally proceeds at a continuously, exponentially decreasing rate. As plotted in Figures 7 and 8, the dissociation rate of CH_4 hydrate followed an approximately linear, negatively sloped trend for up to 80% dissociation. The experiments performed at the lowest *T* and 0.1 MPa (Fig. 7a) were an exception, as the peak in dissociation rate did not occur immediately following depressurization. This dissociation "induction period" showed significantly slower rates for the first 10% of dissociation. In the experiments above 214 K, as well as at 283 K (Fig. 7b), the apparently slower rate for the first 10% of dissociation is an artifact of the time lapse between depressurization and the opening of the line to the flow meter and arises because dissociation rates are high. In all other ex-

periments, the dissociation rates decreased monotonically upon destabilization.

Methane evolution curves (e.g., Figs. 3b and 4b) were fit to a simple power equation to provide a quantitative appraisal of how the rate changes with time, P, and T. We selected an equation that will reproduce the approximately linear trends shown in Figures 7 and 8, but we attach no particular physical significance to the form of the equation. The dissociation experiments reported here were not designed to measure an intrinsic hydrate dissociation rate. In our relatively large, porous samples, mass and heat transport are important factors affecting dissociation below and above the ice melting point, respectively. Such transport issues, discussed in greater depth below, are likely relevant to CH_4 hydrate in natural settings.

The CH_4 evolution curves were fit to a simple power equation of the form:

$$\text{Evolved gas (\%)} = A \cdot t^B \quad (1)$$

where A and B are empirical constants and time t, the independent variable, is in seconds. While the exponent B is independent of the unit of time used, the pre-exponential term A has units of percents s^{-B} and scales non-linearly if the unit of time is changed. The rate of dissociation is then defined as

$$\text{Rate (\% s}^{-1}) = A \cdot B \cdot t^{B-1} \quad (2)$$

In logarithmic form Equation 2 becomes

$$\log (\text{rate}) = \log (A \cdot B) + (B-1) \log (t). \quad (3)$$

This yields a straight line with intercept log ($A \cdot B$) and slope ($B - 1$) (compare to Figs. 7 and 8). Most of the dissociation experiments summarized in Figures 6–8 have been fit to Equation 1. Only experiments performed for at least 20 h (slow rates) or that had reached greater than 60% dissociation (faster rates) were modeled. In experiments that neared or reached complete dissociation at isothermal conditions, the last 5–15% of the reaction was not included in the fit because the rates had decreased well below the trends shown in Figures 7 and 8.

Equation 1 reproduces the dissociation curves reasonably well (within ±5%) for most experiments (Fig. 10), especially given the range in measured rates, and the fit is consistently excellent at 268 K (within ±1%). Both the pre-exponential term A and the exponent B show systematic trends with T that shift abruptly at the boundaries of the anomalous preservation regime (Figs. 10a and 10b). The pre-exponential term A reflects the initial amount of dissociation after 1 s, and the effects of T and P are dramatically enhanced when a larger unit of time is used. The exponential term B, which is between 0 and 1 for all curve fits except two at the lowest temperatures (≤210 K), reflects the decrease in rate over time (see Eq. 3). Its value is distinctly bounded at the anomalous preservation regime boundaries, where abrupt increases occur on either side (Fig. 10b). Note also that the two experiments performed at 204 K, 0.1 MPa yielded different parameters due to differences in dissociation induction times (Fig. 7a) and curve shape. The effects of increasing intergranular porosity in the hydrate, adding quartz sand, and partially satu-

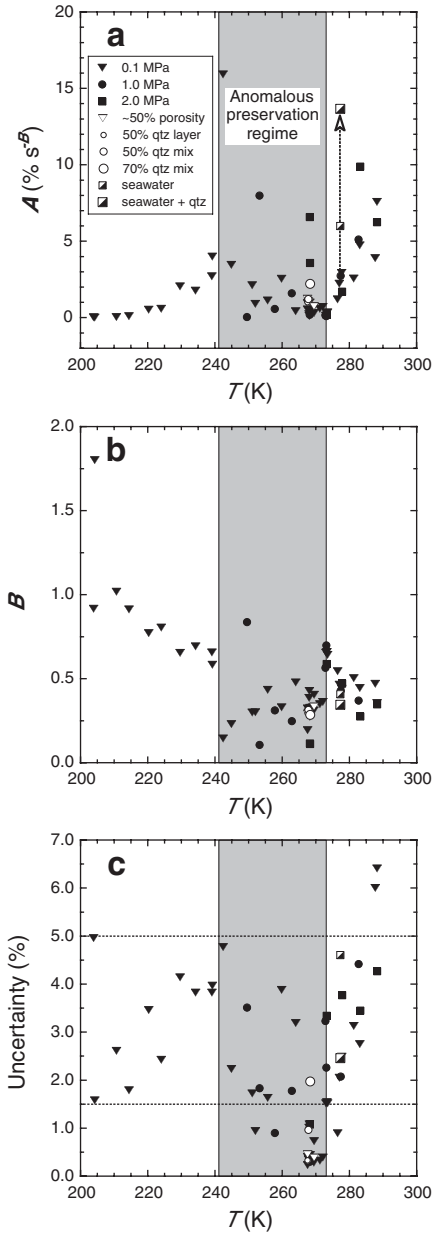

FIGURE 10. Variation with T of the fitting parameters A_0 (**a**), B (**b**), and the uncertainties (**c**) in the expected gas yield obtained from fitting the dissociation data 1 at 0.1 MPa and elevated pressures to Equation. The calculated uncertainties for the fit using Equation 1 (**d**) are typically between 1.5 and 5%. The fit is poorest near the transition to the anomalous preservation regime and at the highest T investigated, where initial dissociation rates are extremely high. Equation 1 does an excellent job of fitting the dissociation curves obtained near 268 K, where dissociation rates are the lowest. The effects of increasing porosity, the addition of quartz sand, and the partial saturation of the porosity with seawater on the fitting parameters are also shown (see text). Note that we have omitted the fitting results to the experiment at 288 K, 0.1 MPa that yielded the highest dissociation rate (see Fig. 6) because the result was not reproducible, required data extrapolation, and yielded inconsistent fitting results. The standard errors for A_0 and B are less than the symbol height.

rating the hydrate with seawater are also reflected in the fitting parameters (Fig. 10).

The form of Equation 1 is the only one that we have been able to apply with reasonable success to the entire data set. The difference between the calculated and observed amount of dissociation is not evenly distributed about the curves (i.e., χ^2 is large), except for data collected in the anomalous preservation regime. But Equation 1 does provide some predictive capabilities for porous CH_4 hydrate in contact with a CH_4 gas phase. There is interdependency between A and B, where a high value for A correlates with a low value for B. The variability in the rate of dissociation is reflected primarily in the pre-exponential term, as the primary variation in the curves in Figures 7 and 8 is their vertical position and not their slope. However, Equation 1 does not have direct physical significance or relationship to the mechanisms of CH_4 hydrate dissociation under various P, T conditions. This topic is given further consideration below.

Dissociation mechanisms for CH_4 hydrate

To summarize, anywhere from less than 5% to more than 90% of a porous CH_4 hydrate sample can persist after a few hours at P, T conditions outside the hydrate stability field. While dissociation rates decrease systematically with increasing pressure, the T-dependency is highly variable and complex over the range investigated (204 to 289 K). As mentioned above, both heat and mass transport are significant factors affecting the dissociation rate of porous CH_4 hydrate under certain conditions, and clearly more than one mechanism must account for the observed range in dissociation behavior.

Methane hydrate dissociation behavior is well-described at temperatures above the ice melting point, where hydrate dissociates to gas + water. At pressures below the quadrupole point, defined where the ice/water boundary intersects the hydrate equilibrium boundary (273.1 K, 2.6 MPa; Fig. 2), samples dissociate to completion within hours, and the dissociation rates increase with increasing T_{ext} (Circone et al. 2000; Figs. 6, 7b, and 8). Upon depressurization and the onset of dissociation, internal sample temperatures decrease to just below the ice melting point, regardless of T_{ext}, and remain buffered there as the reaction proceeds. The rate of dissociation is proportional to the heat flow into the sample (Circone et al. 2000; Peters et al. 2000). Because heat flow may be anisotropic, it must be considered when comparing experimentally determined rates. We have hypothesized that thermal buffering is due to the freezing of the water product, which offsets the larger enthalpy of dissociation to gas + water, and that the T offset from the pure H_2O melting point is due to the presence of dissolved gas product in the water product prior to freezing (Circone et al. 2004). At conditions above the quadrupole point, dissociation also proceeds to completion; however, sample temperatures are buffered at the hydrate equilibrium boundary. Nonetheless, heat transport will govern dissociation rates in macroscopic samples at P, T conditions in the gas + water field (see Fig. 2).

Below the ice melting point, the picture is not as clear. From the equilibrium boundary up to ~240 K at 0.1 MPa, dissociation produces gas + ice, rates increase with increasing T_{ext}, and internal sample temperatures are depressed in proportion to the rate of dissociation but are not buffered at a fixed, reproducible T (Stern et al. 2001). The amount of T overstep of the hydrate equilibrium boundary and heat transport factor into the dissociation rates. However, dissociation does not go directly to completion, but stalls at ≥90%, at which point gas release effectively stops. Several researchers have suggested that the presence of abundant ice product may form a physical barrier to gas diffusion (e.g., Ershov and Yakushev 1992; Davidson et al. 1986; Handa 1986), thus stalling dissociation before 100% reaction occurs. The remaining gas is released easily as samples are warmed, with a distinct, final pulse of gas released as sample temperature reaches the ice melting point. This also points to the presence of ice affecting mass transport under these conditions.

However, in the anomalous preservation region, rates are dramatically depressed within –30 K of the ice melting point, and dissociation stalls when *most* of the CH_4 hydrate remains. Rates are depressed by several orders of magnitude (Figs. 7c, 7d, 8a, 8b), continue to decrease over time, and more than half of the hydrate sample may persist for hundreds of hours. Increasing intergranular porosity, as well as the introduction of other phases (quartz sand, seawater), increases dissociation rates in a systematic manner, suggesting that dissociation in this regime relies on hydrate grain-grain contacts and may also be path-dependent. Thus, in systems where hydrate is a minor component or where it forms a thin layer on another substrate, these anomalously slow dissociation rates may not be observed.

As we have discussed previously (Stern et al. 2001, 2003), the mere presence of an "impermeable" ice layer does not sufficiently explain several aspects of observed hydrate dissociation behavior in this temperature interval: (1) The complex temperature-dependence of CH_4 hydrate dissociation, and the sharp transition in behavior at ~240 to 250 K. (2) The lack of comparable preservation of CH_4 hydrate at lower T. (3) The inverse relationship between greater CH_4 hydrate preservation and ice-layer thickness. (4) The occurrence of optimum CH_4 hydrate preservation near 268 K, where ice is extremely weak (Durham and Stern 2001). (5) The absence of preservation of sII CH_4-C_2H_6 hydrate at 268 K, for which the T-overstep of the equilibrium boundary is even less (Stern et al. 2003). (6) The lack of T-dependent dissociation behavior for sI CO_2 hydrate below 273 K, which attains only 20% dissociation until the ice point is reached, regardless of the P, T pathway followed (Circone et al. 2003).

To date, a satisfactory mechanism that explains this temperature-dependent behavior peculiar to sI CH_4 hydrate has been elusive. For the reasons cited above, the simplest explanation—that the mere presence of ice provides a sufficient diffusional boundary that retards dissociation—is not sufficient, although we do not rule out that ice does play a role. Certainly, these hydrates do not persist once the ice melting point is reached (Circone et al. 2004). At the conditions of the anomalous preservation regime, the formation of a quasi liquid layer on ice may become an important factor. Studies on ice growth (Mason et al. 1963) indicate that surface water mobility is highly temperature-dependent in a range that closely coincides with that for anomalous preservation, but the connection remains purely speculative. Two lines of evidence support a scenario in which water mobility may play some role in preserving CH_4 hydrate in this temperature range: (1) SEM photomicrographs of partially dissociated CH_4 hydrate quenched in liquid N_2 after several hours to days at 268 K, 0.1

MPa, show that, compared to starting material pore textures (Stern et al. 2004), the pore surfaces of anomalously preserved samples are densely recrystallized into minimal surfaces (e.g., Fig. 3 in Stern et al. 2003). Surface recrystallization is not observed in samples dissociated at lower temperatures, which have a spongy, porous texture (Fig. 5 in Stern et al. 2003). (2) At low temperatures, where water mobility is low, formation of gas-release pathways along fractures would permit dissociation to occur more easily. We have performed experiments in which samples were partially dissociated near 250 K, 0.1 MPa, then cooled to 188 K and reheated to 282 K (Stern et al. 2001). The amount of time spent at low temperature (15 vs. 173 minutes) affected the amount of gas released within 30 K of the equilibrium boundary (193 K) vs. at 273 K. Specifically, the longer the sample was held at 188 K, the greater the gas release at low temperature when the sample was later warmed. This hints at the possibility that the low temperature treatment allows development of crack formation and gas-release pathways. Conversely, when samples that were depressurized in the anomalous preservation thermal regime were cycled to and from other temperatures still within the regime, the expected dissociation rates were in all cases recovered (Fig. 2 in Stern et al. 2003).

An additional point that must be addressed is the role that the guest molecule plays. Temperature-dependent dissociation behavior appears to be unique to CH_4 hydrate, based on the gas hydrate compositions that we have investigated to date. CO_2 hydrate, also sI, does not show any of the *T*-dependent behavior below 273 K (Circone et al. 2003), while a sII CH_4-rich hydrate shows no anomalous preservation at 268 K. This suggests that some aspect of the guest molecule is important, but the governing factor (size, shape, or the polar nature of the guest molecule) is not apparent. The dissociation behaviors of various hydrates of both sI and sII are not easily categorized, complicating the role free water and ice may play in the rate of hydrate dissociation under various *P*, *T* conditions.

ACKNOWLEDGMENTS

We acknowledge W.B. Durham, I-M. Chou, and two anonymous reviewers for their helpful comments on the manuscript. We also thank the National Energy Technology Laboratory for supplying supplemental funding through the National Methane Hydrate R&D Program that made possible some of the experiments reported here. J. Pinkston (USGS, Menlo Park) integrated the Tescom back pressure regulator into our existing gas hydrate synthesis/dissociation apparatus and provided additional technical support.

REFERENCES CITED

Circone, S., Stern, L.A., Kirby, S.H., Pinkston, J.C., and Durham, W.B. (2000) Methane hydrate dissociation rates at 0.1 MPa and temperatures above 272 K. In G. Holder and P. Bishnoi, Eds., Gas Hydrates: Challenges for the Future, p. 544–555. New York Academy of Sciences, New York.

Circone, S., Kirby, S.H., Pinkston, J.C., and Stern, L.A. (2001) Measurement of gas yields and flow rates using a custom flowmeter. Review of Scientific Instruments, 72, 2709–2716.

Circone, S., Stern, L.A., Kirby, S.H., Durham, W.B., Chakoumakos, B.C., Rawn, C.J., Rondinone, A.J., and Ishii, Y. (2003) CO_2 hydrate: synthesis, composition, structure, dissociation behavior, and a comparison to structure I CH_4 hydrate. Journal of Physical Chemistry B, 107, 5529–5539.

Circone, S., Stern, L.A., and Kirby, S.H. (2004) The role of water in gas hydrate dissociation. Journal of Physical Chemistry B, 108, 5747–5755.

Dallimore, S.R. and Collett, T.S. (1995) Intrapermafrost gas hydrates from a deep core hole in the Mackenzie Delta, Northwest Territories, Canada. Geology, 23, 527–530.

Davidson, D.W., Garg, S.K., Gough, S.R., Handa, Y.P., Ratcliffe, C.I., Ripmeester, J.A., and Tse, J.S. (1986) Laboratory analysis of a naturally occurring gas hydrate from sediment of the Gulf of Mexico. Geochimica et Cosmochimica Acta, 50, 619–623.

Durham, W.B. and Stern, L.A. (2001) Rheological properties of water ice—applications to satellites of the outer planets. Annual Review of Earth and Planetary Science, 29, 295–330.

Ershov, E.D. and Yakushev, V.S. (1992) Experimental research on gas hydrate decomposition in frozen rocks. Cold Regions Science and Technology, 20, 147–156.

Handa, Y.P. (1986) Calorimetric determinations of the composition, enthalpies of dissociation, and heat capacities in the range 85 to 270 K for clathrate hydrates of xenon and krypton. Journal of Chemical Thermodynamics, 18, 891–902.

——— (1988) A calorimetric study of naturally occurring gas hydrates. Industrial and Engineering Chemistry Research, 27, 872–874.

Handa, Y.P. and Stupin, D. (1992) Thermodynamic properties and dissociation characteristics of methane and propane hydrates in 70 Å radius silica gel pores. Journal of Physical Chemistry, 96, 8599–8603.

Mason, B.J., Bryant, G.W., and Van den Heuvel, A.P. (1963) The growth habits and surface structure of ice crystals. Philosophical Magazine, 8, 744–755.

Peters, D., Selim, M.S., and Sloan, E.D. (2000) Hydrate dissociation in pipelines by two-sided depressurization. In G. Holder and P. Bishnoi, Eds., Gas Hydrates: Challenges for the Future, p. 304–313. New York Academy of Sciences, New York.

Sloan, E.D. (1998) Clathrate Hydrates of Natural Gases, 2nd ed., 705 p. Marcel Dekker, Inc., New York.

Stern, L.A., Kirby, S.H., and Durham, W.B. (1996) Peculiarities of methane clathrate hydrate formation and solid-state deformation, including possible superheating of water ice. Science, 273, 1843–1848.

Stern, L.A., Kirby, S.H., Durham, W.B., Circone, S., and Waite, W.F. (2000) Synthesis of pure methane hydrate suitable for measurement of physical properties and decomposition behavior. In M.D. Max, Ed., Natural Gas Hydrate: In Oceanic and Polar Subaerial Environments, p. 323–349. Kluwer, Dordrecht.

Stern, L.A., Circone, S., Kirby, S.H., and Durham, W.B. (2001) Anomalous preservation of pure methane hydrate at 1 atm. Journal of Physical Chemistry B, 105, 1756–1762.

——— (2003) Temperature, pressure, and compositional effects on anomalous or "self" preservation of gas hydrates. Canadian Journal of Physics, 81, 271–283.

——— (2004) Application of scanning electrons microscopy to investigate growth and annealing of gas clathrate hydrates formed from melting ice. American Mineralogist, 89, 1162–1175

Yakushev, V.S. and Istomin, V.A. (1992) Gas-hydrates self-preservation effect. In N. Maeno and T. Hondoh, Eds., Physics and Chemistry of Ice, 136–139. Hokkaido University Press, Sapporo.

MANUSCRIPT RECEIVED OCTOBER 10, 2003
MANUSCRIPT ACCEPTED APRIL 7, 2004
MANUSCRIPT HANDLED BY BRYAN CHAKOUMAKOS